FINAL REPORT

Title:
The Integration of Theoretical and Experimental Alloy Design in the Development and Testing of a Cast Steel Hammer.

Prepared for: Steel Founders' Society of America

By:

Andrew Balog

Ameen Bello

Grant Hellmich

Aaron Kucera

Austin Whitt

March 2021


TPM
Precision Investment Castings
Sugar Land, Texas

Executive Summary

We began preparing for the competition by researching alloys that have desirable properties for a hammer, this research provided us with 6 main candidates, ASTM 2330, ASTM 4340 and ASTM 5160 steels and H13, S1, S7 tool steels. Heat treating the casted alloy was a very important task to ensure that the properties of the hammer will meet specifications that we desire. By calculating TTT diagrams using Thermocalc and MUCG83 we determined that ASTM steel-4340 was the best candidate, as it presents desired mechanical properties, has sensible heat treatment processes, and can form microstructures with high bainite and martensite concentrations. The design of the hammer was created using Solidworks to draft models and run finite element analysis. The main conditions for the designs were to minimize stress concentrations and subsequent failure, in addition to, constraining the weight to the 6 pound limit. The final design is a scaled down solid hammer which had minimal stress concentrations and failure during simulations. Texas Precision Metalcraft (TPM) acted as our industrial partner as well as sponsored the casting of the hammer head. Their foundry provided us with the cast by method of investment casting which allowed for near net shape parts. After casting, heat treatment was performed by SEI Heat Treat and the final parts were paired with a pecan hickory wooden handle.

1. Background

This project is performed in conjunction with Texas Precision Metalcraft (herein referred to as TPM), a specialty casting company located in Sugarland, Texas. TPM is a "job-based shop", meaning that they work individually with each customer to create a part and processing pathway that meets the customer's specific needs. Investment casting produces parts with much higher dimensional tolerances and smoother surface finishes than other casting processes [1].

2. Methods

Alloy Design

TPM uses prealloyed billets for their casting process. They have the ability to add small amounts of additional elements to modify the composition slightly, but we need a standardized billet to work from. The alloy design section of the project began by examining the most common steels used in commercial hammers. This would allow us to determine good candidates for which base alloy to use. Initially we identified 2000-series nickel steels, 4000-series molybdenum steels, 5000-series chromium steels, and H and S-class tool steels.

The first step in selecting a base alloy was to compare the bulk modulus, hardness, and fracture toughness of the candidate alloys. Bulk modulus is the volumetric version of elastic modulus and relates compressive force to elastic deformation. High bulk modulus indicates a greater ability to recover from deformation caused during a hammer strike. Hardness is a measure of a material's ability to resist plastic deformation. High hardness helps the material to resist permanent deformation. Fracture toughness is the stress intensity factor needed to propagate a fine crack. Having a high fracture toughness results in cracks blunting before propagation and prevents the part from failing by breakage. *Table 1* shows the mechanical properties collected for each alloy initially considered. Collectively, these parameters correspond to greater force required to dent or chip the hammer head.

After conducting an initial literature review, we removed 2000-series steels and 5000-series steels for shortcomings in material properties. Next, a more in-depth literature review was conducted on the remaining 4 steels. The goal of this literature review was to go beyond looking for basic property values, and examine the effects of microstructure, processing conditions, and heat treatments on the steel's properties of interest. The remaining steels were analyzed using Thermo-Calc and MUCG83 to determine which of the options would be best suited for heat treatment to form the desired microstructure. Using this

software, Time-Temperature-Transformation (TTT) diagrams were created. The alloys were then compared on the basis of their tendency to form the desired phases. The metrics used were temperature range and time until the transformation starts. Ideally, the transformation finish time would be compared as well, but MUCG83 cannot calculate this value.

Hammer Design

The first step of our hammer design process was to examine traditional Norse and modern hammer designs. Considering the competition weight limit, our goal was to adopt a style that resembled Mjolnir in Norse mythology while adapting it to a modern sledgehammer size and shape. In the end our designs followed the Marvel studios adaptation of Mjolnir with a cuboid body. This was done to root our designs in a commonly recognizable "Thor" style. After completing our background research, the hammer design process took three distinct stages. The first stage was designing a version of Mjolnir that held similar proportions to that of Marvel's adaptation while reducing the total weight to fit the competition constraints. This first hammer design is shown in *Figure 5* and depicts a solid block of steel on a representative wooden handle. After completing the design, a theoretical performance baseline was set by performing SolidWorks finite element analysis. The simulation was set up to apply force to the front face of the hammer while keeping the handle in a fixed position. This was done to represent the force transferred to the handle when the hammer strikes a surface. After setting a baseline, the next stage was to challenge ourselves as engineers and develop the design to remove wasted material that added to the total weight while providing minimal benefit to mechanical properties. *Figure 6* presents the second stage design with a cross section view. The internal dumbbell shape of this design presented a strong mechanical advantage over the first design in finite element analysis while the external shell maintained a recognizable appearance. This design was initially the favorite but presented many challenges for the casting process as the hollow pockets would be difficult to cast without filling them with material. The final design stage, presented in *Figure 7*, came as the result of realizing the manufacturing challenges associated with the previous design. The final design removed material from the initial solid block design with minimal impact to the mechanical properties observed in the second design. In this final design we also added more detail to the exterior to make the design more easily recognizably "Thor".

During the process of designing the hammer head, we also examined materials for the handle. We wanted to focus weight in the head of the hammer so we looked for a material that had low density and high mechanical properties. Initially we compared carbon fiber, polymers, and hardwoods. After a little research we determined that although carbon fiber has better mechanical properties, the greater density would require pulling too much mass away from the head. On the other hand, we found that polymers had

low densities, but the mechanical properties were not up to our expectations. This led to us focusing our research on hardwoods. *Table 3* presents the specific gravity, modulus of rupture, and specific strength of various woods we examined. Specific gravity is the ratio of a material's density versus a reference substance. Since specific gravity is relative to a reference material, a low specific gravity does not always indicate low density, but it can serve as a means of comparison so long as the reference material remains the same. Modulus of rupture is a measure of a material's bending strength. A high modulus of rupture indicates the material can withstand high bending forces along a plane. For the wood species used in handle design, modulus of rupture is more appropriate than modulus of elasticity because the handle is more likely to be subjected to greater bending stresses than tensile or compressive stresses. Specific strength is the ratio of a material's strength at failure divided by its density. Specific strength allows for better comparison of woods because it adjusts for variations in density. High specific strength shows better ability to withstand applied forces.

Casting Design

After designing the hammer head, a runner system was designed to connect a series of final parts so multiple hammers can be cast in one pour. Seen on the left side in *Figure 1*, this runner system connects multiple replicas of the final part into a central flow system. The addition of each part to the runner creates a larger, single piece instead of multiple individual parts. The number of parts that can be cast from a pattern tree is controlled by the flow of molten metal through the mold. If the volume of the mold is too large some cavities may be underfilled, resulting in useless final parts. Conversely, if the mold is too small, porosity may form in the final parts resulting in underperforming parts. To help prevent poor casting and wasted material, the team consulted with TPM to understand manufacturing techniques used to optimize casting performance.

After conducting 3D modeling and assessing manufacturability, a physical mold was made. Normally molds are made out of wax or polymer, producing a solid pattern tree similar to the one seen on the left side of *Figure 1*. TPM generally uses a wax injection molding process to form molds; this relies on a pre-made mold for the part. This process increases in efficiency as the final number of casted parts increases. Since a pre-made mold would be costly to have manufactured and was impractical for the low number of parts needed for the competition, a stereolithographic (SLA) printed mold was used. TPM helped us partner with Eagle Engineered Solutions, an industrial SLA mold supplier, who could print high quality molds for our needs.

After the polymer wax pattern tree was printed, it was coated with layers of ceramic shell by alternating dipping it into a ceramic slurry and coated it with a layer of ceramic powder. In total 7 dips were

performed. The first 2 dips contained fine grain zircon particles that help to get better surface finish and allow for finer detail. The subsequent 5 dips added layers of coarser material that help strengthen the shell and prevent cracking. Next, the tree was placed into a flash furnace where the temperature was rapidly increased to 1500℉ for 20 minutes. The rapid increase in temperature causes the wax inside to quickly evacuate the mold, leaving a hollow ceramic structure with a smooth inner finish.

Once the wax was removed from the ceramic mold casting was ready to begin. The first step was to load the pattern trees into the oven for preheating. During preheating the molds were loaded into the furnace the night before casting and allowed to heat to 1800℉. This process helps to burnout any remaining wax and ensures when the metal is poured it does not solidify too quickly. While the molds heated up, billets were added to melted at 2900℉ and slag was removed from the melt. Once everything was up to temperature the mold was removed from the furnace and filled with molten metal. Once the mold was full a block of combustible material was added on top and the mold was enclosed in a metal drum. This process is referred to as “can covering” and causes the oxygen in the atmosphere to be burned up, preventing it from leaching carbon from the solidifying metal. This process is often necessary for larger parts approximately the size of our hammer head, that take longer to solidify.

After a few hours the parts had cooled and the molds could be removed from the cans. Once at room temperature, the ceramic mold reverted to being brittle, allowing for the majority of the shell to be removed using a knockout mechanical agitator and steel shot blast. The result was a metal cast of the original wax tree design. Next the parts were machined off the tree using an automatic saw and the remnants of gating were ground down. The final step was to give the parts a caustic clean in a molten salt bath to eat away any remaining shell before sending the parts to SEI Heat Treat for heat treatment.

3. Results and Discussion

Alloy Design

Identification of commonly used steels yielded several categories of steel, namely 2000-series nickel steels, 4000-series molybdenum steels, 5000-series chromium steels, and H and S-classes of tool steels. Common steels used in blacksmithing for tool hammers were researched, as well as some expert advice from mentors, which lead to an initial list consisting of ASTM 2330, ASTM 4340, ASTM 5160, and H13, S1, and S7 tool steels.

ASTM 2330, a 3.5 weight percent Ni steel, was removed early on in the process due to having a significantly lower hardness and fracture toughness compared to the rest of the group (roughly 50%

lower). The ASTM 5160 candidate, a 0.8 weight percent Cr steel, was also discarded early on in the alloy design process due to similar concerns about hardness and fracture toughness.

Further literature review revealed that the ideal microstructure for this application is likely a combination of martensite and bainite due to a combination of high hardness and toughness [4]. This led to H13 steel being removed from consideration as the composition of H13 promotes the formation of carbides which significantly reduce the toughness. Although heat treatments which reduce carbide formation are possible, the other candidates were better suited to form the bainite-martensite microstructure.

Originally, the steels were to be evaluated using TTT diagrams produced by Thermo-Calc. However, Thermo-Calc did not release their updated database for determining the transformation times and temperatures of bainite before we had completed this section of the project. For this reason, MUCG83 was chosen instead. This code was developed by Bhadeshia et al. to model solid state transformation in steels [5]. *Figure 2* compares a TTT diagram produced by Thermo-Calc to one produced by MUCG83 for 4340. The remaining steels were evaluated using MUCG83 to compare how readily they would form the desired microstructure. *Figure 3* shows the TTT diagrams for S1 and S7.

The most important features of the TTT diagrams for the formation of a bainite-rich microstructure are broken down in *Table 2*. S7 has a significantly smaller range between the bainite start and martensite start temperatures, meaning the tempering temperature must be precisely controlled to encourage the formation of bainite. In addition, the bainite transformation takes ten times as long to start in S7 compared to S1 and 4340. For this reason, forming a bainite-rich microstructure in S7 would be slower and more difficult than the other candidates, so S7 was removed from consideration.

Since the remaining two steels had similar mechanical and heat treatment properties the final steel selection was made on the basis of manufacturability. TPM works with 4340 more often than S1 tool steel which increases manufacturing confidence and reliability. For this reason, 4340 steel was selected for casting of the final hammerheads.

A literature review was conducted to determine the ideal heat treatment to produce a bainitic microstructure in 4340 steel with high hardness and toughness. The typical method for forming bainite in steel is to first heat the material until it reaches the austenite phase and then temper at a lower temperature where the transformation to bainite is the most favorable.

Bilal et al. tested the hardness and toughness of 4340 samples tempered at different temperatures for 30, 60, and 90 minutes [6]. *Figure 4* shows the mechanical properties resulting from the different heat treatment schedules. In these tests, the samples tempered at 310℃ were observed to have the highest

toughness and hardness, so 310℃ was chosen for tempering the hammer. 60 minutes of tempering resulted in higher toughness at the expense of some hardness and provided the best properties overall. This led to the overall heat treatment schedule of austenitize at 900℃ for 30 minutes followed by tempering at 310℃ for 60 minutes. The cooling time from 900℃ to 310℃ is not controlled, but the cooling curve can avoid the pearlite region of the graph as long as cooling to 600℃ takes place in around 100 seconds. This would allow the formation of a microstructure consisting of only bainite and martensite.

Hammer Design

In December, the team had selected three possible candidates: a solid scaled down hammer, a dumbbell shaped truss with an outer shell hammer and a weight reduced hammer. These hammer designs have shown the best resistance to strain when tested. *Figure 5* shows an isometric view of the scale hammer. *Figure 6* shows an isometric view of a section of the dumbbell-shelled hammer and an isometric view of the dumbbell-shelled hammer. *Figure 7* shows an isometric view of the final weight reduced hammer, which includes a beveled version of the Mjolnir symbol. The dimensions of all three designs are included in the captions for volume comparison.

The scale hammer, while very easily castable, has the lowest volume of the three. Conversely the dumbbell-shelled hammer, which is the most ideal in volume, came with several issues in casting simulations and was ultimately not chosen due to that fact. The weight reduced hammer was selected to cast due to its balance between castability and volume when compared to the other final options.

The hammer handle material was selected by examining wood, plastic and carbon fiber material properties. We found that while carbon fiber had superior mechanical properties the higher density would require sacrificing hammer weight that should be focused on the head. Plastic handles were removed for the opposite reason as carbon fiber. The low density of polymers was counteracted by poor mechanical properties. Wood was selected for its balance of mechanical properties and moderate density. Additionally, wood is easy to shape and engrave which allows for superior fine detail control. *Table 3* shows a mechanical and physical property comparison of common handle woods. Pecan hickory was selected for the final handle wood because it has a low specific gravity, moderate modulus of rupture, and high specific strength. Pecan hickory is also native to Texas and serves as the state's official tree, adding another layer of symbolism to our design.

Casting Design

At the start of the new year, the designs of the gating and casting tree were designed in Solidworks. *Figure 8* shows an isometric view of the final hammer with two casting gates attached to the bottom, designed with enough thickness and width for the cast to fill before solidification begins. *Figure 9* shows an isometric view of the final tree design with two hammer heads. Traditionally the parts would extend off the sides of a pattern tree, but given the size of the parts and the desired directional solidification, the parts are hung from the bottom.

4. Conclusions

Alloy Design

At the start of the new year, the team selected ASTM 4340 for the final hammer designs. Steel-4340 proved to have the best combination of mechanical properties (Rockwell C hardness, bulk modulus, and fracture toughness) as well as possessing good potential for heat treatment and post-processing. 4340 is also commonly available in bulk samples. Modeling and computation work done via Thermo-Calc and the MUCG83 program has also indicated that 4340 have wide processing ranges to create the microstructure needed for optimal performance. Literature on heat treatment of 4340 led to the decision to temper the material at 310℃ for 60 minutes.

Hammer Design

The hammer design process presented the weight reduced scale hammer as the best bridge between simulation results and manufacturability. The high manufacturability helped to reduce miscasts without sacrificing expected hammer performance. This design is paired with a pecan hickory wood handle that provides resistance to fracture while maximizing mass on the hammerhead. The combination of these two parts will provide the hammer with resistance to damage while optimizing force on the contact surface during a hammer strike.

Casting Design

The casting process was completed with careful consideration at each step. The wax molds were made using precision SLA printing, the ceramic molds were layered to maximize strength leading up to the casting, and casting was performed with every possible precaution. In the end the hammers have a high-quality finish, dimensional accuracy that fits tight with the handle, and post-processing heat treatment was conducted to the specifications we provided.

5. References

1. Pennsylvania Precision Cast Parts. (n.d.). Investment Casting Advantages and Disadvantages. Retrieved October 12, 2020, from http://ppcpinc.com/investment-casting-advantages-disadvantages/
2. CustomPartNet. (2020). Investment Casting [Digital image]. Retrieved October 4, 2020, from https://www.custompartnet.com/wu/investment-casting
3. Dong, Y., Li, X., Zhao, Q., Yang, J., & Dao, M. (2017). Modeling of shrinkage during investment casting of thin-walled hollow turbine blades. Journal of Materials Processing Technology, 244, 190-203.
4. H.K.D.H. Bhadeshia, Bainite in Steels, Institute of Materials, London (1992), 1-450.
5. H.K.D.H. Bhadeshia, A thermodynamic analysis of isothermal transformation diagrams, Metal Science, 16 (1982) 159-165.
6. Mian Muhammad Bilal et al., Effect of austempering conditions on the microstructure and mechanical properties of AISI 4340 and AISI 4140 steels, Journal of Materials Research and Technology, 8, (2016), 5194-5200.

6. Figures and Tables

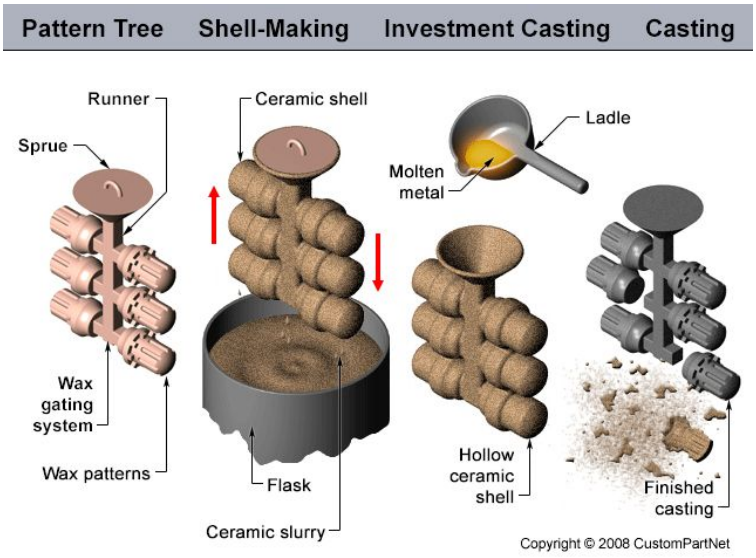

Figure 1. Overview of Investment Casting Process [2].

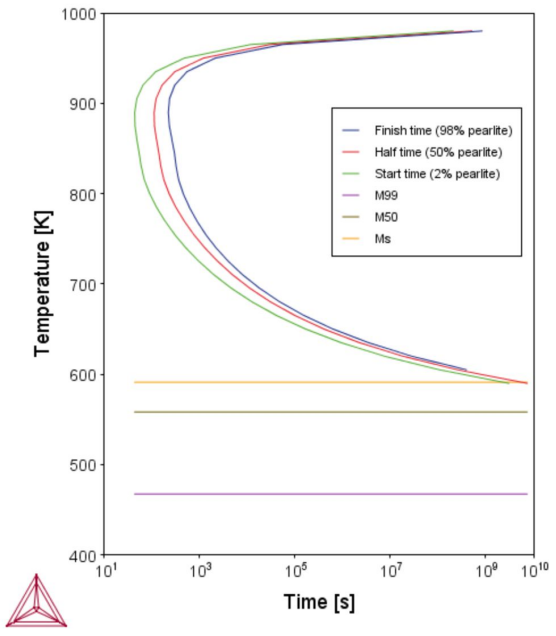

60

Figure 2. TTT diagrams for 4340 steel calculated using Thermo-Calc.

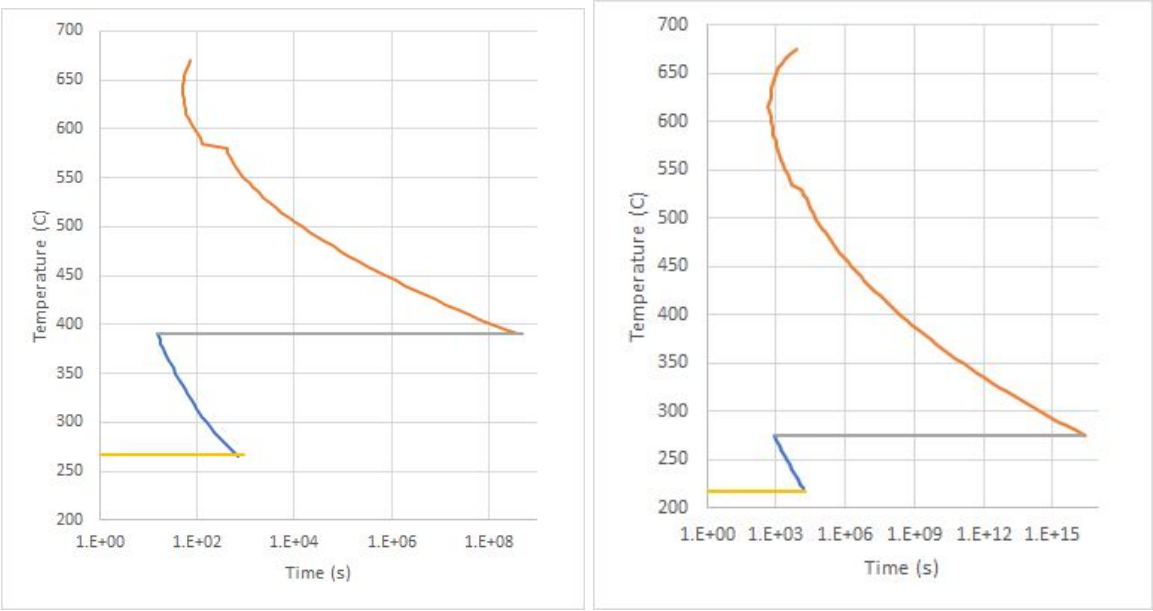

Figure 3. TTT diagrams for S1 steel (left) and S7 steel (right) calculated using MUCG83.

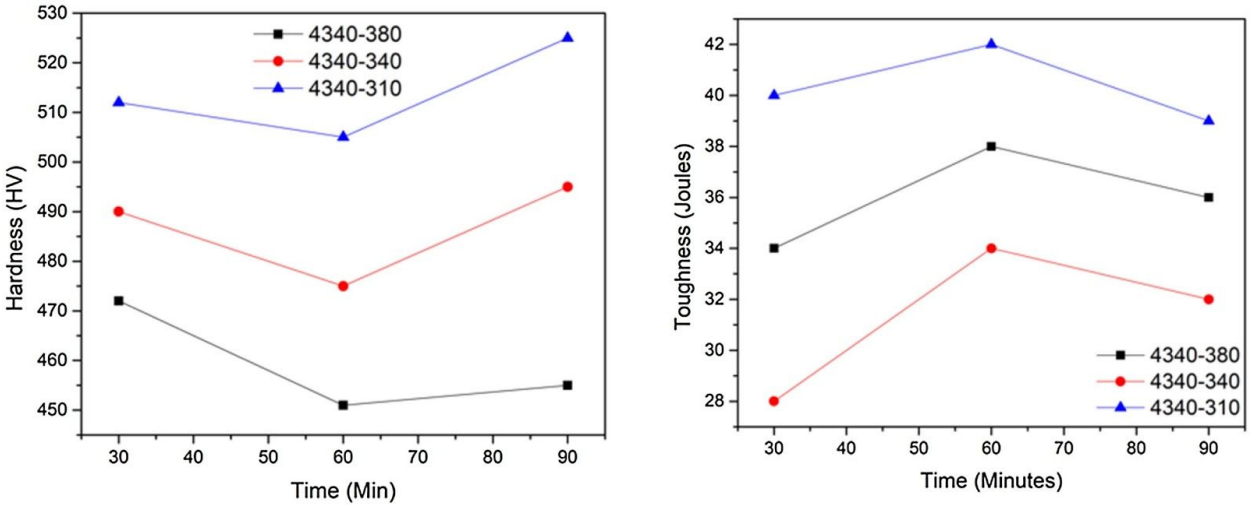

Figure 4. Bilal et al.'s results for the testing of bainitic 4340 steel [6].

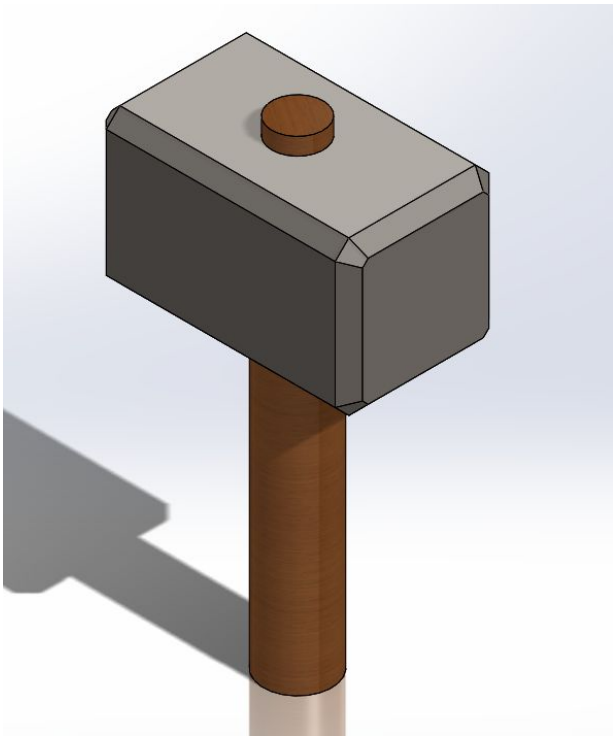

Figure 5. An isometric view of the scale hammer. Dimensions: 2.25” by 3.75” by 7”

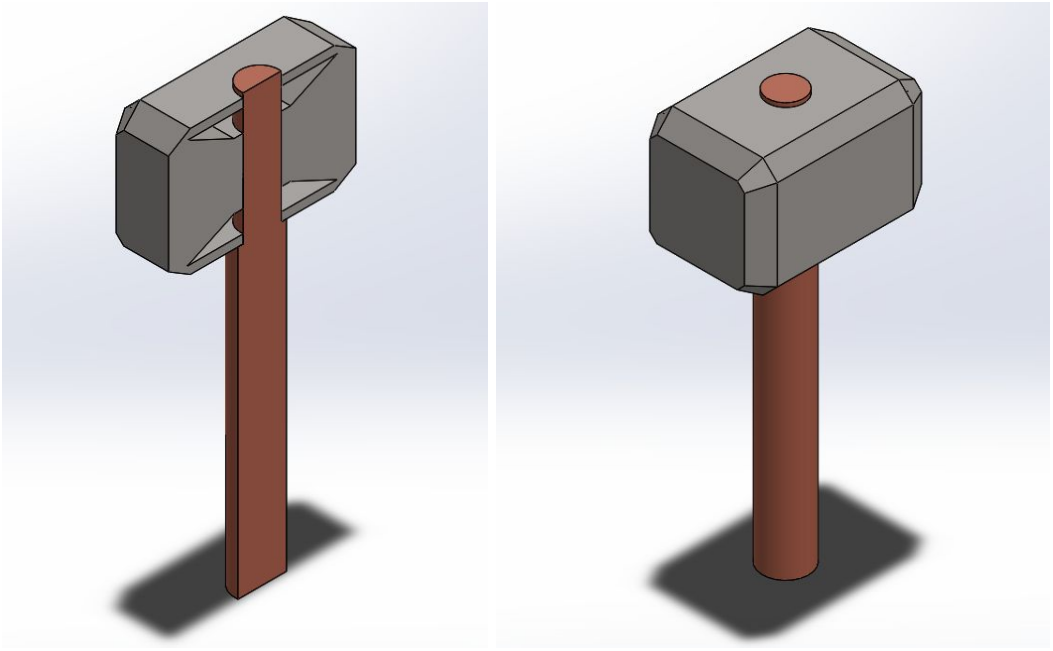

Figure 6. An isometric view of a section of the dumbbell-shelled hammer and an isometric view of the dumbbell-shelled hammer. Dimensions: 2.8” by 4.5” by 10.0”

Figure 7. An isometric view of a section of the weight reduced scale hammer. Dimensions: 2.49” by 4.3” by 10.0”

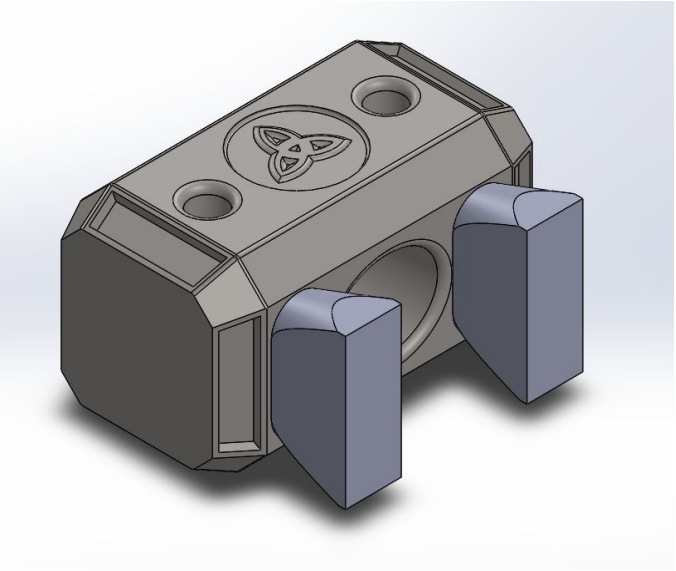

Figure 8. An isometric view of the final hammer design with two casting gates.

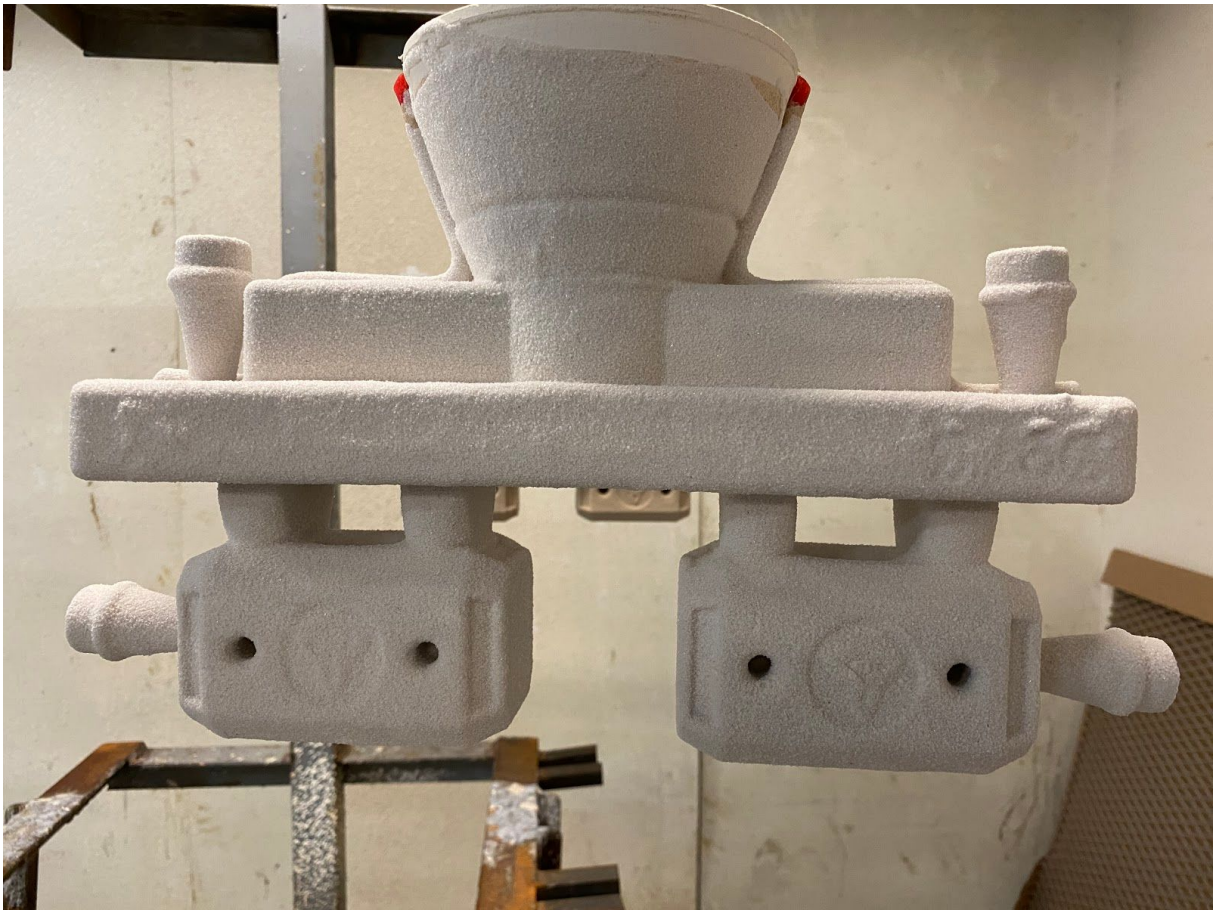

Figure 9. A picture of the final casting tree with two hammer heads, venting system, and casting gates.

Alloy Designation	Hardness (HRC)	Bulk Modulus (GPa)	Fracture Toughness (MPa $m^{1/2}$)
ASTM 2330	25	160 to 170	-
ASTM 4340	40	159	50
ASTM 5160	27	160	23
H13	Up to 54	160	20 to 27
S1	58	160	45
S7	45 to 57	-	47

Table 1. Mechanical properties of candidate alloys.

Alloy	Bs (C)	Ms (C)	Temp Range (C)	Time to start at (Bs+Ms)/2
4340	410	300	110	50s
S1	390	267	123	60s
S7	275	218	57	500s

Table 2. Bainite formation ranges in candidate alloys. Red highlighted values are the areas where S7 showed deficiencies in casting practicality. 4340 is highlighted in green as the alloy selected.

Wood	Specific Gravity	Modulus of Rupture (KPa)	Specific Strength
Yellow Birch	0.62	114	183.87
Hickory (pecan)	0.62	123	198.39
Hickory (true)	0.72	139	193.06
Oak	0.68	125	183.82
Mahogany (true)	0.4	79	197.50

Table 3. Relevant handle wood mechanical and physical properties. Hickory (pecan) is highlighted in green as the handle material selected for the final design.